

ANALYSIS OF STRUCTURE AND MECHANICAL PROPERTIES OF AA 5083 ALUMINIUM ALLOY PROCESSED BY ECAE

N. Llorca-Isern¹, C. Luis-Pérez², P.A. González², L. Laborde¹ and D. Patiño¹

¹CPCM, Dept. Enginyeria Química i Metallúrgia, Fac. Química, Universitat de Barcelona, Martí-Franqués 1-11, 08028 Barcelona, Spain,

² Dept. Ingeniería Mecánica, Energética y de Materiales, Universidad Pública de Navarra, Campus de Arrosadia s/n, 31003 Pamplona, Spain

Received: May 05, 2005

Abstract. In order to alight a little more on the understanding of the mechanisms involved in nanostructuring when severe plastic deformation is carried out by ECAP on ductile alloys, different routes have been applied on a AA 5083 alloy at 423K. Metallographic characterisation has been done by means of optical microscopy, scanning and high resolution transmission electron microscopy to investigate size, morphology, and distribution evolution of the metallic matrix and the precipitates present in this type of aluminium alloy. Also, some mechanical properties have been studied using nanoindentation, US measurements and mechanical testing. From the results it is worth noting that the microstructure shows two observation levels. In one case, as expected, micrometric level does follow classical statements and thus properties are related to microstructure evolution, whereas in the nanometric scale these relationships do not seem to agree.

1. INTRODUCTION

In recent years there has been an increasing interest in the production of ultrafine-grained material for both commercial as well as for research purposes by applying severe plastic deformation processes [1-4]. The equal channel angular pressing or extrusion (ECAP) has been chosen in the present work for the non age-hardenable AA5083 Al alloy. This Al-3%Mg based alloy exhibits interesting mechanical and other physical properties, in particular their remarkable strength and toughness and their potential for superplasticity at low temperatures [5]. However, enhancement of strength by conventional thermal treatment in some non heat-treatable alloys is impossible [6]; thus, the need of

the use of severe plastic deformation methods. The present study examines the changes of structure and mechanical properties of ECAP processed AA5083 by passing up to 11 times through 90° die by Route A (no rotation about sample axis between passes) and up to 4 passes through the same 90° die following Route C (90° rotation about sample axis after each passage through the die). Microstructures were analysed by OM, FE-SEM, TEM and mechanical properties were measured using tensile test, nanoindentation, and US testing.

2. EXPERIMENTAL PROCEDURE

A commercial AA5083 aluminium alloy (Al-4.5%Mg-1.0%Mn-0.15%Cr) supplied in the as-cast state

Corresponding author: N. Llorca-Isern, e-mail: nullorca@ub.edu

material was selected for the ECAE process. Before being processed, the billets were machined to cylindrical samples of 10 mm in diameter and 100 mm in length. The ECAE processing was carried out at a press speed of 50 mm min⁻¹ and at 423K in air to restraint recrystallization using a circular cross-section die with an angle $\Phi = 90^\circ$ and $\psi \sim 10^\circ$ that produces a deformation of $\epsilon \sim 1.05$ on each passage through the die. One set of rods was subjected to 4 passes of ECAP by route C, at which the sample after each pass is rotated along a longitudinal axis by 180° , thus in our specimens processed to a complete cycle. Another set of rods was extruded by route A in which the sample is removed from the die and the extrusion is repeated without any rotation until 11 passes. The initial microstructure and its evolution through ECAP were examined using optical and electron microscopes, S-4100 Hitachi Field emission scanning electron microscope (FEG-SEM) operating at 30 kV and CM-30 Philipps high resolution transmission electron microscope (HRTEM) operated at 300 kV. The foils for TEM observation were prepared from the discs at the centre of specimen and were thinned by dual ion-beam milling (Gatan). The density of dislocations (m⁻²) in TEM imaging was estimated using Ham and Sharp

method [7] consisting of line-dislocations intercept counting:

$$\rho = 2N/Lt, \quad (1)$$

where N is the number of intercept, L is the total lines length (m) and t is the foil thickness; t is calculated using Hirsch method [8]. Tensile tests at room temperature, Vickers hardness, and nanoindentation testing were carried out from samples cut at the centre of the specimen.

3. RESULTS AND DISCUSSION

3.1. Microstructure of AA5083 before ECAP

The initial microstructure of the as-cast AA5083 consisted of equiaxed grains with an average size of about 100 μm (Figs. 1a and 1b) in which the dendritic segregation structure is clearly seen. It is worth noting that from inspection of the as-received sample, coarse precipitates of $(\text{Fe, Mn})_3\text{SiAl}_{12}$ and small Mg_2Si particles are present in the alloy as second-phase. Longitudinal section micrograph is shown in Fig. 1c where similar features to transverse section can be observed. TEM analysis of the undeformed state (Figs. 1d and 1e) showed high

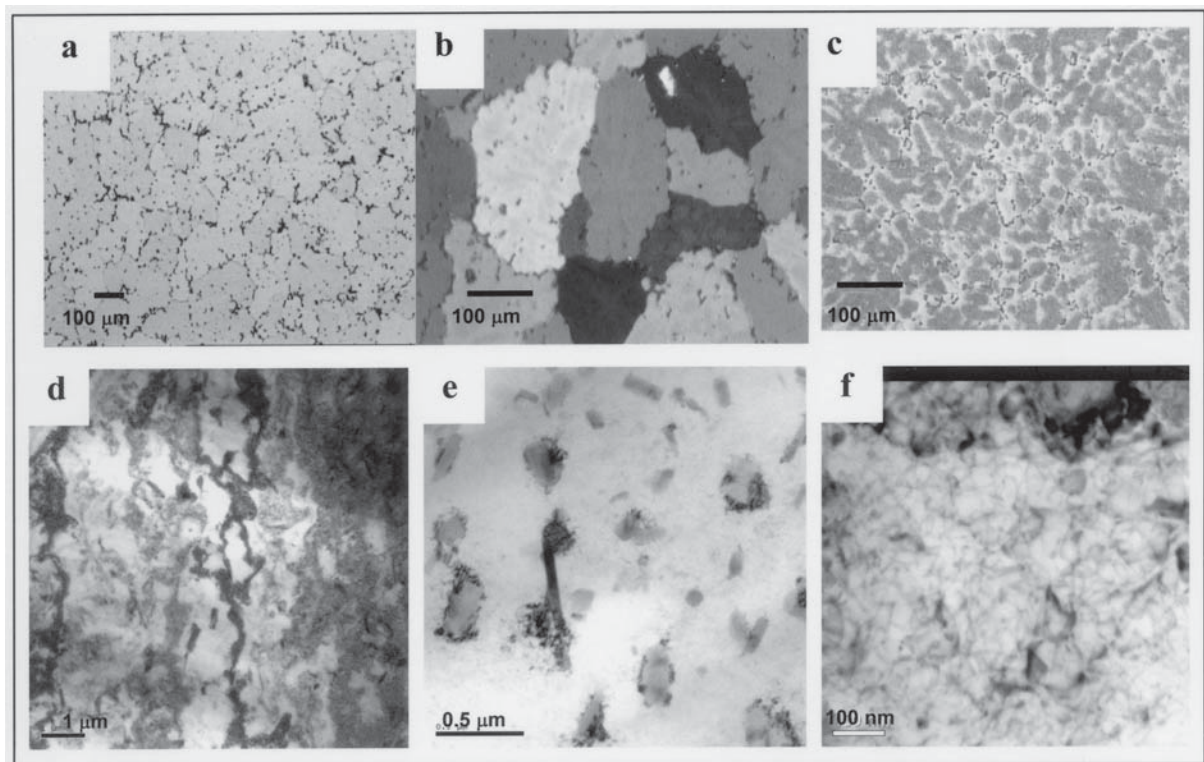


Fig. 1. Initial microstructure of AA5083 as-cast Al alloy: (a), (b) optical micrographs of the transverse central section of the rod, (c) optical micrographs of the longitudinal section of the rod, (d), (e), (f) TEM micrographs at different magnification.

dislocation density distribution (Fig. 1f) resulting from the casting process, the calculated value from Eq. (1) is $\rho = 1.7 \cdot 10^{14} \text{ m}^{-2}$.

3.2. Microstructure of AA5083 after ECAP

General details of the microstructure obtained after deformation by ECAP for 4 passes following route C of the AA5083 aluminium alloy are presented in Fig. 2. After this level of strain, the microstructure shows an inhomogeneous elongated and refined structure (Figs. 2a and 2b). Fig. 2c corresponds to the longitudinal centred section of the deformed sample. When comparing to Fig. 1c, grains appeared more irregular and segregation seems to diminish or also to become more uniform. Tangled dislocations as well as some banded zones can be seen from TEM images of the investigated alloy (Figs. 2d-2f). The original equiaxed as-cast grains are deformed and have adopted a layered structure in which some high deformed grains seem to envelop areas which look not as much deformed. Different slip systems are involved during the deformation process resulting in a deformed inhomogeneous structure and, as observed by other authors in other

aluminium alloys [9,10], with two different strained zones (Figs. 2d and 2e) as they can move as function of differences in lattice rotation between close parts of the crystal. Also this mechanism is enhanced by the presence of different size second phase particles in the AA5083 alloy as well as by the existence of segregated areas that difficult coherent deformation process inside the crystal complicating accommodation of the material. As expected, a notably increased in dislocation density (ρ is about $3.15 \cdot 10^{14} \text{ m}^{-2}$) appears within the grains resulting from the higher irregular strain. No lack of cohesion at particle-matrix interface has been detected. Low angle grain boundaries (LAB) are the dominant feature encountered in the specimen.

Another set of specimens were ECAP processed at 423K following route A until 11 passes. As can be seen in the Fig. 3a, the processing to these high strains leads to the formation of a complete deformation structure in both transverse (Fig. 3a) and longitudinal (Figs. 3b and 3c) sections. In addition, second phase particles are completely broken and oriented to the shear direction (Fig. 3d), also it is worth noting that in some areas, high strain conducted to the matrix-precipitate interface decohesion (Fig. 3e). This fact has only been detected for the

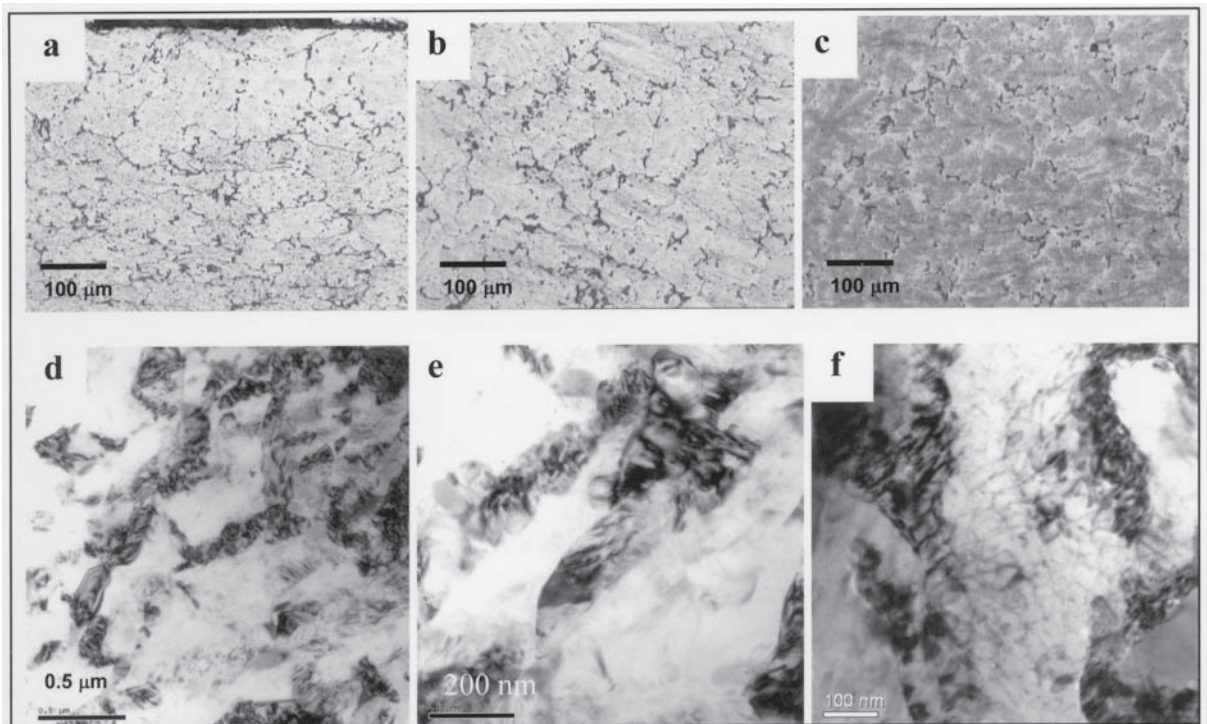


Fig. 2. Microstructure of AA5083 Al alloy after 4 passes through ECAE following Route C: (a), (b) optical micrographs of the transverse central section of the rod, (c) optical micrographs of the longitudinal section of the rod, (d), (e), (f) TEM micrographs of the partially elongated grains at different magnification.

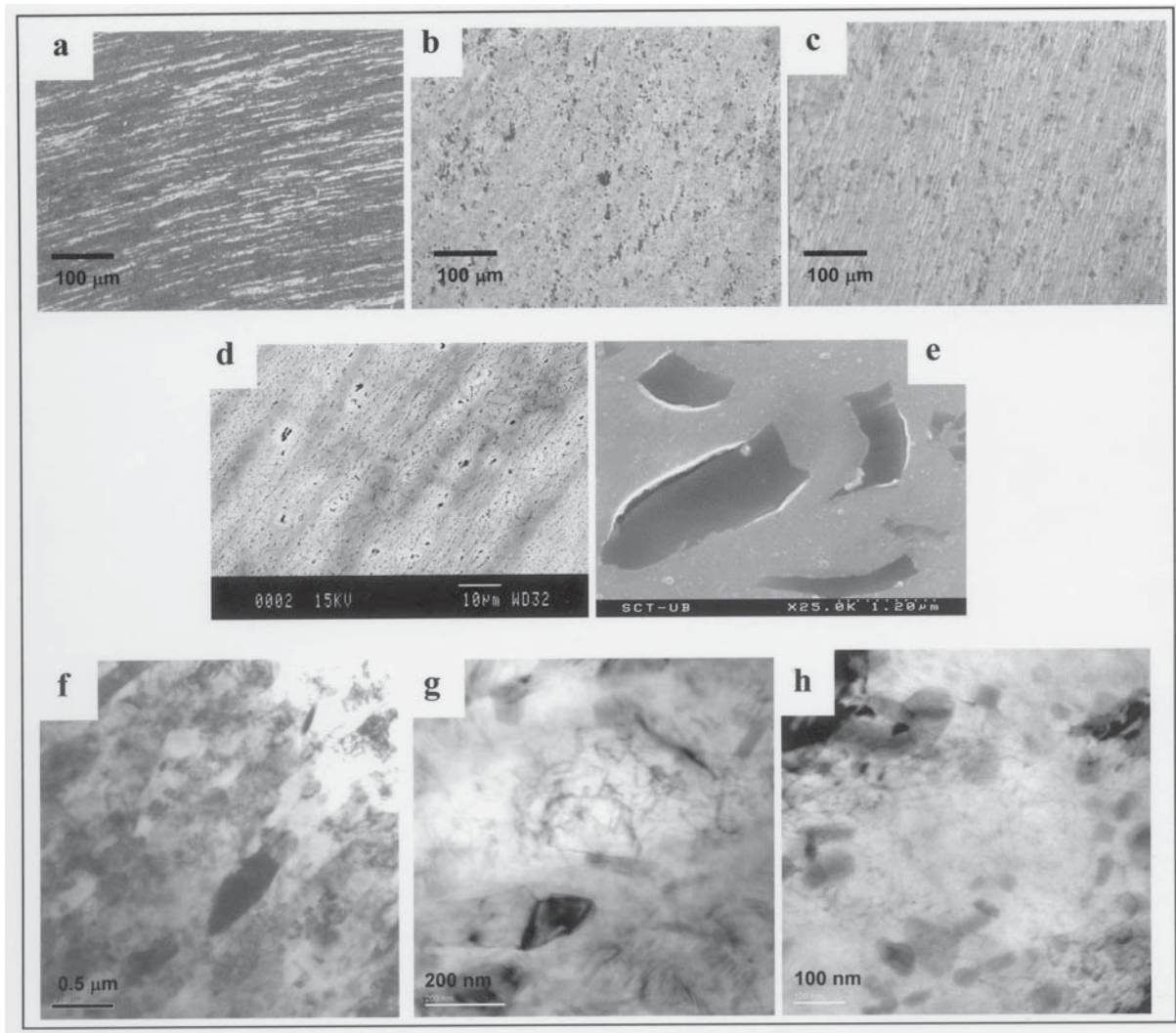


Fig. 3. Microstructure of AA5083 Al alloy after 11 passes through ECAE following Route A: (a) optical micrographs of the highly deformed transverse central section of the rod, (b), (c) optical micrographs of the highly deformed longitudinal section of the rod, (d), (e) SEM micrographs showing the broken precipitates and their orientation in the shear direction (f), (g), (h) TEM micrographs of the deformed grains at different magnification.

initial coarse $(\text{Fe,Mn})_3\text{SiAl}_{12}$ particles. In spite of this, a certain homogeneity in the structure is reached as can be observed in TEM figures. Furthermore, the calculated dislocation density decreases to $1.35 \cdot 10^{14} \text{ m}^{-2}$. Low angle grain boundaries (LAB) are the dominant feature encountered for this set of specimens.

3.3. Mechanical behaviour of ECAP AA5083

Tensile properties were obtained for the as-cast AA5083 and for 8 passes processed by route A

specimens of AA5083 Al alloy. Unfortunately, each ECAPped specimen only provided material for one single tensile test. Taken this into account, the results of the tensile test could have given a dispersion that has been impossible to evaluate. Despite this fact, the tendency is clear and it was found that much improvement in strength was obtained for the processed alloys. One ECAE pass (route A) almost triplicate the strength of the alloy and the latter increased with further passes. The ductility showed by this processed alloy is significantly higher after the second pass through the ECAE and steadily increases with further passes.

Table 1. Hardness measurements for AA5083 Al alloy before and after ECAP processing at 423K.

VICKERS	AA5083-ar 4 passes	AA5083-routeC	AA5083- route A 11 passes
MACROHARDNESS	85. 11 ±2.00	267,20 ±2,89	226,88 ±1,11

Table 2. Tensile tests for AA5083 Al alloy ECAP at 423K.

Number of passes route A 90°angle die	Yield strength (MPa)	Ductility (%)
0 (as-cast)	110	16.6
1	300	–
2	321	19.3
4	345	19.4
6	358	–
8	394	19.6

If we now compare the results of both ECAE routes (Table 1), hardness is higher for the processed samples specially for the specimens pressed following route C. They showed higher macrohardness than specimens processed 11 passes by route A. Elastic constants obtained from nanoindentation tests carried out on the three set of samples (as cast, AA5083-R4, AA5083-A11) showed different characteristics depending on the processing route, nevertheless the Elastic modulus remains constant. Elastic dynamic modulus was obtained by measuring it with NDT Ultrasonic equipment in order to evaluate this property with the lower interaction with the

sample, see Table 2. As other authors suggested, measurements correlate very well with E_{dyn} obtained by mechanical testing equipments [11], see Table 3. This indicates that the stiffness of the specimens did not vary resulting from the accommodation of different effects in the samples as is observed in their structure. Nevertheless, at the very locally nanoindenter measured area, total indentation depths showed the higher resistance of the specimens as well as the elastic energy involved in the test when loading and unloading up to 1000 mN which is more important for the ECAE processed specially the one processed following route C. Also the plastic energy decreases and the plastic resistance is doubled comparing to the as-cast specimen

4. SUMMARY

ECAP is effective hi introducing a high density of dislocations in as-cast Al 5083 alloy depending on the route imposed for deformation. Route C seems more effective than Route A for strengthened the alloy. Nevertheless, if the number of passes following Route A is high, the energy involved in the straining process can damage coarse second phase precipitates causing decohesion in the precipitate-matrix interface. A high tensile ductility (over

Table 3. Elastic constants from nanoindentation tests and Elastic Dynamic Modulus (E_{dyn}) from NOT Ultrasound testing.

	Wt (nJ)	We (nJ)	Wr (nJ)	$E/(1-\nu^2)$ (GPa)	H_{plast} (N/mm ²)	hr' (mm)	E (GPa)	V	E_{dyn} (GPa)
AA5083	2363,00	253,50	2109,17	59,58	851,17	6,67	73.33	0.35	75.78
As-received	±33.53	±19.54	±23.77	±5.70	±35.89	±0.14	±5.00		
AAS083	1790,60	304,60	1485,60	68,44	1609,20	4,85	77.85	0.35	75.5S
Route C	±24.66	±9.92	±31.34	±2.51	±23.12	±0.04	±2.21		
4 passes									
AA5083 Route A	1784,50	266,00	1518,50	78,90	1514,00	5.00	86.31	0.34	5.71
11 passes	±3.54	±14.14	±10.61	±5.09	±19.80	±0.03	±4.47		

strength through strain hardening is obtained by pressing by ECAE at 423K. An accommodation and rearrangement of dislocations network takes place together with the fact that high angle boundaries (HAB) are seldom seen, thus its behaviour may be interpreted by considering precipitates as well as dislocation cell boundaries but not only due to the influence of HAB. ECAE processing also contributes not only to refine material grain size but also significantly modifying the precipitates morphology as well as their distribution which results in a banded microstructure and an elongated distribution of very fine grains.

REFERENCES

- [1] R.Z. Valiev, N.A. Krasilnikov and N.K. Tsenev // *Mat.Sci. Eng. A* **137** (1991) 35.
- [2] V.M.Segal // *Mat.Sci. Eng. A* **197** (1995) 157.
- [3] Y.Wang, M.Chen, F.Zhou and E.Ma // *Nature* **419** (2002) 912.
- [4] N.A.Krasilnikov, W.Lojkowski, Z.Pakiela and R.Z. Valiev // *Mat.Sci. Eng. A* **397** (2005) 330.
- [5] R.X. Hecht, K. Kannan, In: *Superplasticity and Superplastic Forming*, ed. by A.K.Gosh and T.R.Bieler (IMS: Warrendale, 1995) p.259.
- [6] *Metals Reference Book*, ed. M.Baucchio (ASM: Materials Park, 1993) p.614.
- [7] P.K.Ham and N.G.Sharp // *Phil.Mag.* **6** (1961) 1183.
- [8] P.B.Hirsh, In: *Electron Microscopy of Thin Crystals*, ed. by P.B.Hirsh, KB.Nicholson, A. Howie, D.W.Pashley and M. J.Whelan (Butterworths: London, 1965) p.532.
- [9] R.Kaibyshev, K.Shilipova, F.Musin and Y.Motohashi // *Mat. Sci. Eng. A* **396** (2005) 341.
- [10] M.A. Munoz-Morris, C.Garcia Oca, G.Gonzalez Doncel and D.G.Morris // *Mat. Sci. Forum* **426-432** (2003) 2643.
- [11] I. Fonseca, J.A. Benito, I. Megia, A Roca and J. Jorba // *Rev. Met.* **38** (2002) 249.